Strathprints Institutional Repository

Dielectronic Recombination of Fe XV forming Fe XIV: Laboratory Measurements and Theoretical Calculations

D. V. Lukić[1], M. Schnell[2], and D. W. Savin

Columbia Astrophysics Laboratory, Columbia University, New York, NY 10027, USA

lukic@astro.columbia.edu

C. Brandau[3], E. W. Schmidt, S. Böhm[4], A. Müller, and S. Schippers

Institut für Atom- und Molekülphysik, Justus-Liebig-Universität, D-35392 Giessen, Germany

M. Lestinsky, F. Sprenger, and A. Wolf

Max-Planck-Institut für Kernphysik, D-69117 Heidelberg, Germany

Z. Altun

Department of Physics, Marmara University, Istanbul 81040, Turkey

and

N. R. Badnell

Department of Physics, University of Strathclyde, G4 0NG Scotland, UK

ABSTRACT

We have measured resonance strengths and energies for dielectronic recombination (DR) of Mg-like Fe XV forming Al-like Fe XIV via $N = 3 \rightarrow N' = 3$ core excitations in the electron-ion collision energy range 0–45 eV. All measurements were carried out using the heavy-ion Test Storage Ring at the Max Planck Institute for Nuclear Physics in Heidelberg, Germany. We have also carried out new

[1]On leave from the Institute of Physics, 10001 Belgrade, Serbia

[2]Present address, Carl Zeiss NTS GmbH, Oberkochen D-73447, Germany

[3]Present address, Gesellschaft für Schwerionenforschung (GSI), Darmstadt, D-64291, Germany

[4]Present address, Department of Atomic Physics, Stockholm University, S-106 91 Stockholm, Sweden

multiconfiguration Breit-Pauli (MCBP) calculations using the AUTOSTRUCTURE code. For electron-ion collision energies $\lesssim 25$ eV we find poor agreement between our experimental and theoretical resonance energies and strengths. From 25 to 42 eV we find good agreement between the two for resonance energies. But in this energy range the theoretical resonance strengths are $\approx 31\%$ larger than the experimental results. This is larger than our estimated total experimental uncertainty in this energy range of $\pm 26\%$ (at a 90% confidence level). Above 42 eV the difference in the shape between the calculated and measured $3s3p(^1P_1)nl$ DR series limit we attribute partly to the nl dependence of the detection probabilities of high Rydberg states in the experiment. We have used our measurements, supplemented by our AUTOSTRUCTURE calculations, to produce a Maxwellian-averaged $3 \rightarrow 3$ DR rate coefficient for Fe XV forming Fe XIV. The resulting rate coefficient is estimated to be accurate to better than $\pm 29\%$ (at a 90% confidence level) for $k_{\rm B}T_e \geq 1$ eV. At temperatures of $k_{\rm B}T_e \approx 2.5 - 15$ eV, where Fe XV is predicted to form in photoionized plasmas, significant discrepancies are found between our experimentally-derived rate coefficient and previously published theoretical results. Our new MCBP plasma rate coefficient is $19 - 28\%$ smaller than our experimental results over this temperature range.

Subject headings: atomic data – atomic processes – plasmas – galaxies: active – galaxies: nuclei – X-rays: galaxies

1. Introduction

Recent Chandra and XMM Newton X-ray observations of active galactic nuclei (AGNs) have detected a new absorption feature in the 15-17 Å wavelength range. This has been identified as an unresolved transition array (UTA) due mainly to $2p - 3d$ inner shell absorption in iron ions with an open M-shell (Fe I - Fe XVI). UTAs have been observed in IRAS 13349+2438 (Sako et al. 2001), Mrk-509 (Pounds et al. 2001), NGC 3783 (Blustin et al. 2002; Kaspi et al. 2002; Behar et al. 2003), NGC 5548 (Steenbrugge et al. 2003), MR 2251-178 (Kaspi et al. 2004), I Zw 1 (Gallo et al. 2004), NGC 4051 (Pounds et al. 2004), and NGC 985 (Krongold et al. 2005).

Based on atomic structure calculations and photoabsorbtion modeling, Behar et al. (2001) have shown that the shape, central wavelength, and equivalent width of the UTA can be used to diagnose the properties of AGN warm absorbers. However, models which fit well absorption features from second and third row elements cannot reproduce correctly the observed UTAs due to the fourth row element iron. The models appear to predict too high

an ionization level for iron. Netzer et al. (2003) attributed this discrepancy to an underestimate of the low temperature dielectronic recombination (DR) rate coefficients for Fe M-shell ions. To investigate this possibility Netzer (2004) and Kraemer et al. (2004) arbitrarily increased the low temperature Fe M-shell DR rate coefficients. Their model results obtained with the modified DR rate coefficients support the hypothesis of Netzer et al. (2003). New calculations by Badnell (2006a) using a state-of-the-art theoretical method disscused in § 5 further support the hypotesis of Netzer et al. (2003).

Astrophysical models currently use the DR data for Fe M-shell ions recommended by Arnaud & Raymond (1992). These data are based on theoretical DR calculations by Jacobs et al. (1977) and Hahn (1989). The emphasis of this early theoretical work was on producing data for modeling collisional ionization equilibrium (sometimes also called coronal equilibrium). Under these conditions an ion forms at a temperature about an order of magnitude higher than the temperature where it forms in photoionized plasmas (Kallman & Bautista 2001). The use of the Arnaud & Raymond (1992) recommended DR data for modeling photoionized plasmas is thus questionable. Benchmarking by experiment is highly desirable.

Reliable experimentally-derived low temperature DR rate coefficients of M-shell iron ions are just now becoming available. Until recently, the only published Fe M-shell DR measurements were for Na-like Fe XVI (Linkemann et al. 1995; Müller 1999; here and throughout we use the convention of identifying the recombination process by the initial charge state of the ion). The Na-like measurements were followed up with modern theoretical calculations (Gorczyca & Badnell 1996; Gu 2004; Altun et al. 2007). Additional M-shell experimental work also exists for Na-like Ni XVIII (Fogle et al. 2003) and Ar-like Sc IV and Ti V (Schippers et al. 1998, 2002). We have undertaken to measure low temperature DR for other Fe M-shell ions. Our results for Al-like Fe XIV are presented in Schmidt et al. (2006) and Badnell (2006b). The present paper is a continuation of this research.

DR is a two-step recombination process that begins when a free electron approaches an ion, collisionally excites a bound electron of the ion and is simultaneously captured into a Rydberg level n. The electron excitation can be labeled $Nl_j \rightarrow N'l'_{j'}$ where N is the principal quantum number of the core electron, l its orbital angular momentum, and j its total angular momentum. The intermediate state, formed by simultaneous excitation and capture, may autoionize. The DR process is complete when the intermediate state emits a photon which reduces the total energy of the recombined ion to below its ionization limit.

In this paper we present experimental and theoretical results for $\Delta N{=}N' - N = 0$ DR of Mg-like Fe XV forming Al-like Fe XIV. In specific we have studied $3 \rightarrow 3$ DR via the

resonances:

$$\mathrm{Fe}^{14+}(3s^2[^1\mathrm{S}_0]) + e^- \rightarrow \begin{cases} \mathrm{Fe}^{13+}(3s3p[^3P^o_{0,1,2};\ ^1P_1]nl) \\ \mathrm{Fe}^{13+}(3s3d[^3D_{1,2,3};\ ^1D_2]nl) \\ \mathrm{Fe}^{13+}(3p^2[^3P_{0,1,2};\ ^1D_2;\ ^1S_0]nl) \\ \mathrm{Fe}^{13+}(3p3d[^3D^o_{1,2,3};\ ^3F^o_{2,3,4};\ ^3P^o_{0,1,2};\ ^1P^o_1;\ ^1D^o_2;\ ^1F^o_3]nl) \\ \mathrm{Fe}^{13+}(3d^2[^3P_{0,1,2};\ ^3F_{2,3,4};\ ^1D_2;\ ^1G_4;\ ^1S_0]nl) \end{cases} \quad (1)$$

Possible contributions due to $3s3p\ ^3P$ metastable parent ions will be discussed below. Table 1 lists the excitation energies for the relevant Fe XV levels, relative to the ground state, that have been considered in our theoretical calculations. In our studies we have carried out measurements for electron-ion center-of-mass collision energies $E_{\rm cm}$ between 0 and 45 eV.

Our work is motivated by the "formation zone" of Fe M-shell ions in photoionized gas. This zone may be defined as the temperature range where the fractional abundance of a given ion is greater than 10% of its peak value (Schippers et al. 2004). We adopt this definition for this paper. Savin et al. (1997, 1999, 2002a,b, 2006) defined this zone as the temperature range where the fractional abundance is greater than 10% of the total elemental abundance. This is narrower than the Schippers et al. (2004) definition. For Fe XV the wider definition corresponds to a $k_BT_e \approx$ 2.5-15 eV (Kallman & Bautista 2001). It should be kept in mind that this temperature range depends on the accuracy of the underlying atomic data used to calculate the ionization balance.

The paper is organized as follows: The experimental arrangement for our measurements is described in § 2. Possible contamination of our parent ion beam by metastable ions is discussed in § 3. Our laboratory results are presented in § 4. In this section the experimentally-derived DR rate coefficient for a Maxwellian plasma is provided as well. Theoretical calculations which have been carried out for comparison with our experimental results are discussed in § 5. Comparison between the experimental and theoretical results is presented in § 6. A summary of our results is given in § 7.

2. Experimental Technique

DR measurements were carried out at the heavy-ion test storage ring (TSR) of the Max-Planck Institute for Nuclear Physics (MPI-K) in Heidelberg, Germany. A merged beams technique was used. A beam of $^{56}\mathrm{Fe}^{14+}$ with an energy of 156 MeV was provided by the MPI-K accelerator facility. Ions were injected into the ring and their energy spread reduced using electron cooling (Kilgus et al. 1990). Typical waiting times after injection and before measurement were $\approx$ 1 s. Mean stored ion currents were $\approx$ 10 μA. Details of

the experimental setup have been given elsewhere (Kilgus et al. 1992; Lampert et al. 1996; Schippers et al. 1998, 2000, 2001).

Recently a second electron beam has been installed at the TSR (Sprenger et al. 2004; Kreckel et al. 2005). This allows one to use the first electron beam for continuous cooling of the stored ions and to use the second electron beam as a target for the stored ions. In this way a low velocity and spatial spread of the ions can be maintained throughout the course of a DR measurement. The combination of an electron cooler and an electron target can be used to scan energy-dependent electron-ion collision cross sections with exceptional energy resolution. In comparison to the electron cooler, the electron source and the electron beam are considerably smaller and additional procedures, such as the stabilization of the beam positions during energy scans and electron beam profile measurements, are required to control the absolute luminosity product between the ion and electron beam on the same precise level as reached at the cooler. The target electron beam current was ≈ 3 mA. The beam was adiabatically expanded from a diameter of 1.6 mm at the cathode to 7.5 mm in the interaction region using an expansion factor of 22. This was achieved by lowering the guiding magnetic field from 1.28 T at the cathode to 0.058 T in the interaction region thus reducing the transverse temperature to approximately 6 meV. The relative electron-ion collision energy can be precisely controlled and the recombination signal measured as a function of this energy. We estimate that the uncertainty of our scale for $E_{\rm cm}$ is $\lesssim 0.5\%$.

The electrons are merged and demerged with the ion beam using toroidal magnets. After demerging, the primary and recombined ion beams pass through two correction dipole magnets and continue into a bending dipole magnet. Recombined ions are bent less strongly than the primary ion beam and they are directed onto a particle detector used in single particle counting mode. Some of the recombined ions can be field-ionized by motional electric fields between the electron target and the detector and thus are not detected. Here we assumed a sharp field ionization cutoff and estimated for Fe XV that only electrons captured into $n_{\rm max} \lesssim 80$ are detected by our experimental arrangement.

The experimental energy distribution can be described as a flattened Maxwellian distribution. It is characterized by the transversal and longitudinal temperatures $T_\perp$ and $T_\parallel$, respectively. The experimental energy spread depends on the electron-ion collision energy and can be approximated according to the formula $\Delta E = ([\ln(2) k_{\rm B} T_\perp]^2 + 16 \ln(2) E_{\rm cm} k_{\rm B} T_\parallel)^{1/2}$ (Pastuszka et al. 1996). For the comparison of our theoretical calculations with our experimental data we convolute the theoretical results described in § 5 with the velocity distribution function given by Dittner et al. (1986) to simulate the experimental energy spread.

With the new combination of an electron target and an electron cooler we obtain in the present experiment electron temperatures of $k_B T_\perp \approx 6$ meV and $k_B T_\parallel \approx 0.05$ meV. In order

to verify the absolute calibration of the absolute rate coefficient scale we also performed a measurement with the electron cooler using the previous standard method (Kilgus et al. 1992, Lampert et al. 1996). We find consistent rate coefficients and spectral shapes, while the electron temperatures were larger by a factor of about 2 with the electron cooler alone. Moreover, because of the large density of resonances found in certain regions of the Fe XV DR spectrum the determination of the background level for the DR signal was considerably more reliable in the higher resolution electron target data than in the lower resolution cooler data. Hence, we performed the detailed analysis presented below on the electron target data only.

Details of the experimental and data reduction procedure are given in Schippers et al. (2001, 2004) and Savin et al. (2003) and reference therein. The baseline experimental uncertainty (systematic and statistical) of the DR measurements is estimated to be $\pm 25\%$ at a 90% confidence level (Lampert et al. 1996). The major sources of uncertainties include the electron beam density determination, ion current measurements, and corrections for the merging and demerging of the two beams. Additional uncertainties discussed below result in a higher total experimental uncertainty as is explained in §§ 3 and 4. Unless stated otherwise all uncertainties in this paper are cited at an estimated 90% confidence level.

3. Metastable Ions

For Mg-like ions with zero nuclear spin (such as ^{56}Fe), the $1s^2 2s^2 2p^6 3s3p\ ^3P_0$ level is forbidden to decay to the ground state via a one-photon transition and the multiphoton transition rate is negligible. Hence this level can be considered as having a nearly infinite lifetime (Marques, Parente, & Indelicato 1993; Brage et al. 1998). It is possible that these metastables are present in the ion beam used for the present measurements.

We estimate that the largest possible metastable $^3P_0$ fraction in our stored beam is 11%. This assumes that 100% of the initial Fe^{14+} ions are in ^3P_J levels and that the levels are statistically populated. We expect that the $J = 1$ and 2 levels will radiatively decay to the ground state during the ~ 1 s between injection and measurement. The lifetimes of the $^3P_1$ and $^3P_2$ levels are $\sim 1.4 \times 10^{-10}$ s (Marques et al. 1993) and ~ 0.3 s (Brage et al. 1998), respectively. These decays leave 1/9th or 11% of the stored ions in the $^3P_0$ level.

Our estimate is only slightly higher than the inferred metastable fraction for the ion beam used for DR measurements of the analogous Be-like Fe^{22+} (Savin et al. 2006). The Be-like system has a metastable $1s^2 2s2p\ ^3P_0$ state and following the above logic the stored Be-like ion beam had an estimated maximum 11% $^3P_0$ fraction. Fortunately, for the Be-like

measurements we were able to identify DR resonances due to the $^3P_0$ parent ion and use the ratio of the experimental to theoretical resonance strengths to infer the $^3P_0$ fraction. There we determined a metastable fraction of $7\% \pm 2\%$. A similar fraction was inferred for DR measurements with Be-like Ti^{18+} ions (Schippers et al. 2007).

Using theory as a guide, we have searched our Mg-like data fruitlessly for clearly identifiable DR resonances due to metastable $^3P_0$ parent ions. First, following our work in the analogous Be-like Fe^{22+} with its $2s2p\ ^3P_0 \rightarrow 2p^2$ core excitation channel (Savin et al. 2006), we searched for Fe^{14+} resonances associated with the relevant $3s3p\ ^3P_0 \rightarrow 3p^2$ core excitations. However, most of these yield only very small DR cross sections as they strongly autoionize into the $3s3p\ ^3P_{J=1,2}$ continuum channels. These are energetically open at $E_{\rm cm}$ greater than 0.713 eV and 2.468 eV, respectively (Table 1). Hence, above $E_{\rm cm} \approx 0.713$ eV there are no predicted significant DR resonances for metastable Fe^{14+} via $3s3p\ ^3P_0 \rightarrow 3p^2$ core excitations. Below this energy the agreement between theory and experiment is extremely poor (as can be seen in Fig. 1) and we are unable to assign unambiguously any DR resonance to either the ground state or metastable parent ion. Second, we searched for resonances associated with $3s3p\ ^3P_0 \rightarrow 3s3p\ ^1P_1$, $3s3p\ ^3P_0 \rightarrow 3s3p\ ^3P_1$, and $3s3p\ ^3P_0 \rightarrow 3s3p\ ^3P_2$ core excitation which are energetically possible for capture into the $n \geq 14$, 62, and 33 levels, respectively, and which may contribute to the observed resonance structures. The analogous $2s2p\ ^3P_0 \rightarrow 2s2p\ ^1P_1$ and $2s2p\ ^3P_0 \rightarrow 2s2p\ ^3P_2$ core excitations were seen for Be-like Ti^{18+} (Schippers et al. 2007). However, again the complexity of the Fe XV DR resonance spectrum (cf., Fig. 1) prevented unambiguous identification for DR via any of these three core excitations. Hence despite these two approaches, we have been unable to directly determine the metastable fraction of our Fe^{14+} beam.

Clearly our assumption that the ^3P_J levels are statistically populated is questionable. Ion beam generation using beam foil techniques are known to produce excited levels. The subsequent cascade relaxation could potentially populated the J levels non-statistically (Martinson & Gaupp 1974; Quinet et al. 1999). Additionally the magnetic sublevels m_J can be populated non-statistically (Martinson & Gaupp 1974) which may affect the J levels. However, our argument in the above paragraphs that the ^3P_J levels are statistically populated yields $^3P_0$ fractions of the analgous Be-like Ti^{18+} and Fe^{22+} of 11% while our measurements found metastable fractions of $\sim 7\%$ for those two beams. From this we conclude either (a) that if 100% of the initial ions are in the ^3P_J levels, then the $J = 0$ level is statistically under-populated or (b) that the fraction of initial ions in the ^3P_J levels is less than 100% by a quantity large enough that any non-statistical populating of the various J levels still yields only a 7% $^3P_0$ metastable fraction of the ion beam. Thus we believe that our assumption provides a reasonable upper limit to the metastable fraction of the Fe^{14+} beam.

Based on our estimates above and the Be-like results we have assumed that 6%±6% of the Fe^{14+} ions are in the $3s3p\,^3P_0$ metastable state and the remaining fraction in the $3s^2\,^1S_0$ ground state. Here, we treat this possible 6% systematic error as a stochastic uncertainty and add it in quadrature with the 25% uncertainty discussed above.

4. Experimental Results

Our measured $3 \rightarrow 3$ DR resonance spectrum for Fe XV is shown in Figs. 1 - 8. The data $\langle \sigma v \rangle$ represent the summed DR and radiative recombination (RR) cross sections times the relative velocity convolved with the energy spread of the experiment, i.e., a merged beam recombination rate coefficient (MBRRC).

The strongest DR resonance series corresponds to $3s^2\ ^1S_0 \rightarrow 3s3p\ ^1P_1$ core excitations. Other observed features in the DR resonance spectrum are possibly due to double core excitations discussed in § 1. Trielectronic recombination (TR), as this has been named, has been observed in Be-like ions (Schnell et al. 2003a,b; Fogle et al. 2005). These ions are the second row analog to third row Mg-like ions. However in our data unambiguous assignment of possible candidates for the TR resonances could not be made.

Extracted resonance energies E_i and resonance strengths S_i for $E_{\rm cm} \leq 0.95$ eV are listed in Table 2 along with their fitting errors. These data were derived following the method outlined in Kilgus et al. (1992). Most of these resonances were not seen in any of the theoretical calculations for either ground state or metastable Fe^{14+}. Hence their parentage is uncertain. The implications of this are discussed below.

Difficulties in determining the non-resonant background level of the data contributed an uncertainty to the extracted DR resonance strengths. For the strongest peaks this was on the order of $\approx 10\%$ for $E_{\rm cm} \lesssim 5$ eV and $\approx 3\%$ for $E_{\rm cm} \gtrsim 5$ eV. Taking into account the 25% and 6% uncertainties discussed in §§ 2 and 3, respectively, this results in an estimated total experimental uncertainty for extracted DR resonance strengths of ±28% below ≈ 5 eV and ±26% above.

Due to the energy spread of the electron beam, resonances below $E_{\rm cm} \lesssim k_B T_\perp$ cannot be resolved from the near 0 eV RR signal. Here this limit corresponds to ≈ 6 meV. But we can infer the absence of resonances lying below the lowest resolved resonance at 6.74 meV. For $E_{\rm cm} \lesssim k_{\rm B} T_\parallel$, a factor of up to $\sim 2-3$ enhanced MBRRC is observed in merged electron-ion beam experiments (see e.g., Gwinner et al. 2000; Heerlein et al. 2002). Here this temperature limit corresponds to $E_{\rm cm} \lesssim 0.05$ meV. As shown in Fig. 9, at an energy 0.005 meV our MBRRC is a factor of 2.5 times larger than the fit to our data using the RR cross section

from semi-classical RR theory with quantum mechanical corrections (Schippers et al. 2001) and the extracted DR resonance strengths and energies. This enhancement is comparable to that found for systems with no unresolved DR resonances near 0 eV (e.g., Savin et al. 2003 and Schippers at al. 2004). Hence, we infer that there are no additional significant unresolved DR resonances below 6.74 meV. Recent possible explanations for the cause of the enhancement near 0 eV have been given by Hörndl et al. (2005, 2006) and reference therein.

We have generated an experimentally-derived rate coefficient for $3 \rightarrow 3$ DR of Fe XV forming Fe XIV in a plasma with a Maxwellian electron energy distribution (Fig. 10). For $E_{\rm cm} \leq 0.95$ eV we have used our extracted resonance strengths listed in Table 2. For energies $E_{\rm cm} \geq 0.95$ eV we have numerically integrated our MBRRC data after subtracting out the non-resonant background. The rate coefficient was calculated using the methodology outlined in Savin (1999) for resonance strengths and in Schippers et al. (2001) for numerical integration.

In the present experiment only DR involving capture into Rydberg levels with quantum numbers $n_{\rm max} \lesssim 80$ contribute to the measured MBRRC. In order to generate a total ΔN=0 plasma rate coefficient we have used AUTOSTRUCTURE calculations (see § 5) to account for DR into higher n levels. As is discussed in more detail in § 6, between 25-42 eV we find good agreement between the experimental and AUTOSTRUCTURE resonance energies. However, the theoretical results lie a factor of 1.31 above the measurement. To account for DR into $n \geq n_{\rm max} = 80$, above 42 eV we replaced the experimental data with the AUTOSTRUCTURE results ($n_{\rm max}$ =1000) reduced by a factor of 1.31. Our resulting rate coefficient is shown in Fig. 10.

Including the DR contribution due to capture into $n > 80$ increases our experimentally-derived DR plasma rate coefficient by $< 1\%$ for $k_B T_e < 7$ eV, by $< 2.5\%$ at 10 eV and by $< 7\%$ at 15 eV. This contribution increases to 20% at 40 eV, rises to 27% at 100 eV and saturates at $\approx 35\%$ at 1000 eV. Thus we see that accounting for DR into $n > n_{\rm max} = 80$ levels has only a small effect at temperatures of $k_B T_e \approx$ 2.5-15 eV where Fe XV is predicted to form in photoionized gas (Kallman & Bautista 2001). Also, any uncertainties in this theoretical addition, even if relatively large, would still have a rather small effect at these temperatures on our derived DR total rate coefficient. Hence, we have not included this in our determination below of the total experimental uncertainty for the experimentally-derived plasma rate coefficient at $k_B T_e \geq 1$ eV.

The two lowest-energy resonances in the experimental spectrum occur at energies of 6.74 meV and 9.80 meV with resonance strengths of 1.89×10^{-16} cm^2 eV and 1.01×10^{-17} cm^2 eV, respectively (see Table 1 and Fig. 9). As already mentioned, the parentage for the two lowest energy resonances is uncertain. These resonances dominate the DR

rate coefficient for $k_BT_e < 0.24$ eV. The contribution is 50% at 0.24 eV, 16% at 0.5 eV, 6.5% at 1 eV, 2.4% at 2.5 eV, and $< 0.31\%$ above 15 eV. At temperatures where Fe XV is predicted to form in photoionized plasmas, contributions due to these two resonances are insignificant. Because of this, we do not include the effects of these two resonances when calculating below the total experimental uncertainty for the experimentally-derived plasma rate coefficient at $k_BT_e \geq 1$ eV.

An additional source of uncertainty in our results is due to possible contamination of the Fe XV beam by metastable $^3P_0$ ions. Because we cannot unambiguously identify DR resonances due to metastable parent ions, we cannot directly subtract out any contributions they may make to our experimentally-derived rate coefficient. Instead we have used our AUTOSTRUCTURE calculations for the metastable parent ion as a guide, multiplied them by 0.06 on the basis of the estimated $(6 \pm 6)\%$ metastable content. We then integrated them to produce a Maxwellian rate coefficient and compared the results to our experimental results, leaving out the two lowest measured resonances at 6.74 and 9.80 meV. As discussed in the paragraph above, these two resonaces were left out because of the uncertainty in their parentage and their small to insignificant effects above 1 eV. The metastable theoretical results are 9.5% of this experimentally-derived rate coefficient at $k_BT_e = 1$ eV, 4.9% at 2.5 eV, 2.2% at 5 eV, 1% at 10 eV and $< 0.77\%$ above 15 eV.

In reality these are probably lower limits for the unsubtracted metastable contributions to our experimentally-derived rate coefficient. However, these limits appear to be reasonable estimates even taking into account the uncertainty in the exact value of the contributions due to metastable ions. For example, if we assume that we have the estimated maximum metastable fraction of 11%, then our experimentally-derived rate coefficients would have to reduced by only 9.0% at 2.5 eV, 4.0% at 5 eV, 1.8% at 10 eV, and less than 1.4% above 15 eV. Alternatively, it is likely that theory underestimates the resonance strength for the metastable parent ions similar to the case for ground state parent ions (cf., Fig. 1). However, if the metastable fraction is 6% and the resonance contributions are a factor of 2 higher, then our experimentally-derived rate coefficients would have to reduced by only 9.8% at 2.5 eV, 4.4% at 5 eV, 2.0% at 10 eV, and less than 1.5% above 15 eV. These are small and not very significant corrections. We consider it extremely unlikely that we have underestimated by a factor of nearly 2 both the metastable fraction and the metastable resonance contribution. Thus we expect contamination due to metastable $^3P_0$ ions to have a small to insignificant effect on our derived rate coefficient at temperatures where Fe XV is predicted to form in photoinoized gas.

Taking into account the baseline experimental uncertainty of 25%, the metastable fraction uncertainty of 6%, and the nonresonant background uncertainty of 10%/3%, all dis-

cussed above, as well as the uncertainty due to the possible unsubtracted metastable resonances, the estimated uncertainty in the absolute magnitude of our total experimentally-derived Maxwellian rate coefficient ranges between 26% and 29% for $k_B T_e \geq 1$ eV. Here we conservatively take the total experimental uncertainty to be $\pm 29\%$. This uncertainty increases rapidly below 1 eV due to the ambiguity of the parentage for the two lowest energy resonances and possible resonance contributions from metastable Fe XV which we have not been able to subtract out.

We have fitted our experimentally-derived rate coefficient plus the theoretical estimate for capture into $n > 80$ using the simple fitting formula

$$\alpha_{DR}(T_e) = T_e^{-3/2} \sum_i c_i e^{-E_i/k_B T_e} \tag{2}$$

where c_i is the resonance strength for the ith fitting component and E_i the corresponding energy parameter. Table 3 lists the best-fit values for the fit parameters. All fits to the total experimentally-derived Maxwellian-averaged DR rate coefficient show deviations of less than 1.5% for the temperature range $0.001 \leq k_B T_e \leq 10000$ eV.

In Table 3, the Experiment (I) column gives a detailed set of fitting parameters where the first 30 values of c_i and their corresponding E_i values are for all the resolved resonances for $E_{\rm cm} \leq 0.95$ eV given in Table 2. The parentage for these resonances are uncertain, though the majority are most likely due to ground state and not metastable Fe^{14+}. It is our hope that future theoretical advances will allow one to determine which resonances are due to ground state ions and which are due to metastables. Listing the resonances as we have will allow future researchers to readily exclude those resonances which have been determined to be due to the metastable parent. The remaining 6 fitting parameters yield the rate coefficient due to all resonances for $E_{\rm cm}$ between 0.95 and the $3s3p(^1P_1)nl$ series limit at 43.63 eV. In the Experiment (II) column of Table 3, the first six sets of c_i and E_i give the fitting parameters for the first six resonances. The remaining sets of fit parameters are due to all resonances between 0.1 eV and the series limit.

5. Theory

The only published theoretical DR rate coefficient for Fe XV which we are aware of is the work of Jacobs et al. (1977). Using the work of Hahn (1989), Arnaud and Raymond (1992) modified the results of Jacobs et al. (1977) to take into account contributions from $2p-3d$ inner-shell transitions. The resulting rate coefficient of Arnaud and Raymond (1992) is widely used throughout the astrophysics community.

We have carried out new calculations using a state-of-the-art multiconfiguration Breit-Pauli (MCBP) theoretical method. Details of the MCBP calculations have been reported in Badnell et al. (2003). Briefly, the AUTOSTRUCTURE code was used to calculate energy levels as well as radiative and autoionization rates in the intermediate-coupling approximation. These must be post-processed to obtain the final state level-resolved and total dielectronic recombination data. The resonances are calculated in the independent process and isolated resonance approximation (Seaton & Storey 1976).

The ionic thresholds were shifted to known spectroscopic values for the $3 \rightarrow 3$ transitions. Radiative transitions between autoionizing states were accounted for in the calculation. The DR cross section was approximated by the sum of Lorentzian profiles for all included resonances. The AUTOSTRUCTURE calculations were performed with explicit n values up to 80 in order to compare closely with experiment. The resulting MBRRC is presented for $3 \rightarrow 3$ core excitations in Figs. 1-8.

The theoretical $3 \rightarrow 3$ DR plasma rate coefficient was obtained by convolving calculated DR cross section times the relative electron-ion velocity with a Maxwellian electron energy distribution. Cross section calculations were carried out up to $n_{\max} = 1000$. The resulting Maxwellian plasma rate coefficient is given in Fig. 10.

We have fit our theoretical $3 \rightarrow 3$ MCBP Maxwellian DR rate coefficients using Eq. 2. The resulting fit parameters are presented in Table 3. The accuracy of the MCBP fit is better than 0.5% for the temperature range $0.1 \leq k_B T_e \leq 10000$ eV. This lower limit represents the range over which rate coefficient data were calculated. Data are not presented below $(10^1 z^2)/11605$ eV, which is estimated to be the lower limit of the reliability for the calculations (Badnell 2007). Here $z = 14$ and this limit is 0.17 eV.

6. Discussion

6.1. Resonance Structure

As we have already noted, we find poor agreement between our experimental and theoretical resonance energies and strengths for electron-ion collision energies below 25 eV. Theory does not correctly predict the strength of many DR resonances which are seen in the measurement. A similar extensive degree of disparity between the theoretical and the measured resonances was also seen in our recent Fe^{13+} results (Schmidt et al. 2006; Badnell 2006b).

Some of the weaker peaks in our data below 1 eV may be due to the possible presence

of metastable Fe^{14+} in our beam. But the estimated small metastable contamination seems unlikely to be able to account in this range for many of the strong resonances which are not seen in the present theory. Above $\approx$ 1 eV, we expect no significant DR resonances due to metastable Fe^{14+} (as is discussed in § 3).

In the energy range from $1 - 25$ eV, the differences between experiment and theory are extensive. The reader can readily see from Figs. 1-8 that theory does not correctly predict the strength of many resonances which are observed in the experiment. This conclusion takes into account the by-eye shifting of the theoretical resonances energies to try to match up theory with the measured resonances.

Between $25 - 42$ eV we find good agreement between the experiment and theory for resonance energies. The AUTOSTRUCTURE code reproduces well the more regular resonance energy structure of high-n Rydberg resonances approaching the $3s3p(^1P_1)nl$ series limit. However the AUTOSTRUCTURE cross section lies $\approx 31\%$ above the measurements. This discrepancy is larger than the estimated $\pm 26\%$ total experimental uncertainty in this energy range. A similar discrepancy with theory was found for Fe^{13+} (Badnell 2006b).

Theory and experiment diverge above 42 eV and approaching the $3s3p(^1P_1)nl$ series limit. We attribute the difference in the shape between the calculated and measured $3s3p(^1P_1)nl$ series limit partly to the nl dependence of the field-ionization process in the experiment. Here we assumed a sharp n cutoff. Schippers et al. (2001) discuss the effects of a more correct treatment of the field-ionization process in TSR. Their formalism uses the hydrogenic approximation to take into account the radiative lifetime of the Rydberg level n into which the initially free electron is captured.

Our theoretical calculations indicate there are no DR resonances due to $2 \rightarrow 3$ or $3 \rightarrow 4$ core excitations below 44 eV, significant or insignificant. The two weak peaks above the $3s3p(^1P_1)nl$ series limit at 43.63 eV are attributed to ΔN=1 resonances.

6.2. Rate Coefficients

The recommended rate coefficient of Arnaud & Raymond (1992) is in mixed agreement with our experimental results (Fig. 10). For temperatures below 90 eV, their rate coefficient is in poor agreement. At temperatures where Fe XV is predicted to form in photoionzed gas, their data are a factor of 3 to orders of magnitude smaller than our experimental results. At temperatures above 90 eV, the Arnaud & Raymond (1992) data are in good agreement with our combined experimental and theoretical rate coefficient.

As already implied by the work of Netzer et al. (2003) and Kraemer et al. (2004), the present result shows that the previously available theoretical DR rate coefficients for Fe XV are much too low at temperatures relevant for photoionized plasmas. Other storage ring measurements show similar difference with published recommended low temperature DR rate coefficients for Fe M-shell ions (Müller 1999; Schmidt et al. 2006). The reason for this discrepancy is primarily because the earlier theoretical calculations were for high temperature plasmas and did not include the DR channels important for low temperatures plasmas.

At temperatures relevant for the formation of Fe XV in photoionized gas, we find that the modified Fe XV rate coefficient of Netzer (2004) is up to an order of magnitude smaller than our experimental results. The modified rate coefficient of Kraemer et al. (2004) is a factor of over 3 times smaller. These rate coefficients were guesses meant to investigate the possibility that larger low temperature DR rate coefficients could explain the discrepancy between AGN observations and models. The initial results were suggestive that this is the case. Our work confirms that the previously recommended DR data are indeed too low but additionally shows that the estimates of Netzer et al. (2003) and Kraemer et al. (2004) are also still too low. A similar conclusion was reached by Schmidt et al. (2006) based on their measurement for Fe^{13+}. Clearly new AGN modeling studies need to be carried out using our more accurate DR data (Badnell 2006a).

Our state-of-the-art MCBP calculations are 37% lower than our experimental results at a temperature of 1 eV. This difference decreases roughly linearly with increasing temperature to $\approx$ 25% at 2.5 eV. It is basically constant at $\approx$ 23% up to 7 eV and then again nearly monotonically decreases to 19% at 15 eV. As discussed in § 4, a small part of these difference may be attributed to unsubtracted metastable $^3P_0$ contributions. But these contributions are $< 10\%$ at 2.5 eV, $< 5\%$ at 5 eV, $< 2.0\%$ at 10 eV, and $< 1.4\%$ above 15 eV (hence basically insignificant). Above 15 eV the difference decreases and at 23 eV and up the agreement is within $\lesssim 10\%$ with theory initially smaller than experiment but later greater. Part of the good agreement at these higher temperatures is due to our use of theory for the unmeasured DR contribution due to states with $n > 80$.

7. Summary

We have measured resonance strengths and energies for ΔN=0 DR of Mg-like Fe XV forming Al-like Fe XIV for center-of-mass collision energies $E_{\rm cm}$ from 0 to 45 eV and compared our results with new MCBP calculations. We have generated an experimentally-derived plasma rate coefficient by convolving the measured MBRRC with a Maxwell-Boltzmann electron energy distribution. We have supplemented our measured MBRRC with MCBP cal-

culations to account for unmeasured DR into states which are field-ionized before detection. The resulting plasma recombination rate coefficient has been compared to the recommended rate coefficient of Arnaud & Raymond (1992) and new calculations using a state-of-the-art MCBP theoretical method. We have considered the issues of metastable ions in our stored ion beam, enhanced recombination for collision energies near 0 eV, and field-ionization of high Rydberg states in the storage ring bending magnets.

As suggested by Netzer et al. (2003) and Kraemer et al. (2004), the present result shows that the previously available theoretical DR rate coefficients for Fe XV are much too low. Other storage ring measurements show similar differences with published recommended low temperature DR rate coefficients for M-shell iron ions (Müller 1999; Schmidt et al. 2006). We are now in the process of carrying out DR measurements for additional Fe M-shell ions. As these data become available we recommend that these experimentally-derived DR rate coefficients be incorporated into AGN spectral models in order to produce more reliable results.

We gratefully acknowledge the excellent support by the MPI-K accelerator and TSR crews. CB, DVL, MS, and DWS were supported in part by the NASA Space Astrophysics Research Analysis program, the NASA Astronomy and Astrophysics Research and Analysis program, and the NASA Solar and Heliosperic Physics program. This work was also supported in part by the German research-funding agency DFG under contract no. Schi 378/5.

REFERENCES

Altun, Z., Yumak, A., Yavuz, I., Badnell, N. R., Loch, S. D., & Pindzola, M. S. 2007, in preparation

Arnaud, M., & Raymond, J. 1992, ApJ, 398, 394

Badnell, N. R., et al. 2003 A&A, 406, 1151

Badnell, N. R. 2006a, ApJ, 651, L73

Badnell, N. R. 2006b, J. Phys. B, 39, 4285

Badnell, N. R. 2007, http://amdpp.phys.strath.ac.uk/tamoc/DATA/DR/

Behar, E., Sako, M., & Kahn S. M. 2001, ApJ, 563, 497

Behar, E., et al. 2003, ApJ, 598, 232

Blustin, A. J., et al. 2002, A&A, 442, 757

Brage, T., Judge, P. G., Aboussaied, A., Godefroid, M. R., Joensson, P., Ynnerman, A., Fischer, C. F., & Leckrone, D. S. 1998, ApJ, 500, 507

Churilov, S. S., Levashov, V. E., & Wyart, J. F. 1989, Phys. Scr., 40, 625

Dittner, P. F., Datz, S., Miller, P. D., Pepmiller, P. L., & Fou, C. M. 1986, Phys. Rev. A, 33, 124

Fogle, M., Badnell, N. R., Eklöw, N., Mohamed, T., & Schuch, R. 2003, A&A, 409, 781

Fogle, M., Badnell, N. R., Glans, P., Loch, S. D., Madzunkov, S., Abdel-Naby, Sh. A., Pindzola, M. S., & Schuch, R. 2005, A&A, 442, 757

Gallo, L. C., Boller, T., Brandt, W. N., Fabian, A. C., & Vaughan, S. 2004, A&A, 417, 29

Gorczyca T. W., & Badnell, N. R. 1996, Phys. Rev. A, 54, 4113

Gu, M. F. 2004, ApJ, 589, 389

Gwinner, G., et al. 2000, Phys. Rev. Lett., 84, 4822

Hahn, Y. 1989, J. Quant. Spectrosc. Radiat. Transfer, 41, 315

Heerlein, C., Zwicknagel, G., & Toepffer, C. 2002, Phys. Rev. Lett., 89, 083202

Hörndl, M., Yoshida, S., Wolf, A., Gwinner, G., & Burgdörfer J. 2005, Phys. Rev. Lett., 95, 243201

Hörndl, M., Yoshida, S., Wolf, A., Gwinner, G., Seliger, M., & Burgdörfer J. , Phys. Rev. A 74, 052712

Jacobs, V. L., Davis, J., Kepple, P. C., & Blaha, M. 1977, ApJ, 211, 605

Kallman, T. R., & Bautista M. 2001, ApJS, 133, 221

Kaspi, S., et al. 2002, ApJ, 574, 643

Kaspi, S., Netzer, H., Chelouche, D., George, I. M., Nandra, K., & Turner, T. J. 2004, ApJ, 611, 68

Kilgus, G., et al. 1990, Phys. Rev. Lett., 64, 737

Kilgus, G., Habs, D., Schwalm, D., Wolf, A., Badnell, N. R., & Müller, A. 1992, Phys. Rev. A, 46, 5730

Kraemer, S. B., Ferland, G. J., & Gabel, J. R. 2004, ApJ, 604, 561

Kreckel, H.. et al. 2005, Phys. Rev. Lett., 95, 263201

Krongold, Y., Nicastro, F. M., Brickhouse, N. S., Mathura, S., & Zezas, A. 2005, ApJ, 620, 165

Lampert, A., Wolf, A., Habs, D., Kilgus, G., Schwalm, D., Pindzola, M. S., & Badnell, N. R. 1996, Phys. Rev. A, 53, 1413

Linkemann, J., et al. 1995, Nucl. Instrum. Methods Phys. Res. B, 98, 154

Marques, J. P., Parent, F., & Indelicato, P. 1993, At. Data. Nuc. Data Tab., 55, 157

Martinson, I., & Gaupp, A. 1974, Phys. Rep. 15, 113

Müller, A. 1999, Int. J. Mass Spectrom., 192, 9

Netzer, H., et al. 2003, ApJ, 599, 933

Netzer, H. 2004, ApJ, 604, 551

Nikolić, D., et al. 2004, Phys. Rev. A, 70, 062723

Pastuszka, S., et al. 1996, Nucl. Instrum. Methods Phys. Res. A, 369, 11

Pounds, K. A., Reeves, J. N., O'Brien, P. T., Page, K. A., Turner, M. J. L., & Nayakshin S. 2001, ApJ, 559, 181

Pounds, K. A., Reeves, J., King, A. R, & Page, K. L. 2004, MNRAS, 350, 10

Quinet, P., Palmeri, P., Bimont, E., McCurdy. M. M., Rieger, G., Pinnington, E. H., Wickliffe, M. E., & Lawler, J. E. 1999, Mon. Not. R. Astron. Soc. 307, 934

Ralchenko, Yu., et al. 2006, NIST Atomic Spectra Database (version 3.1.0), [Online]. Available: http://physics.nist.gov/asd3. National Institute of Standards and Technology, Gaithersburg, MD.

Sako, M., et al. 2001, A&A, 365, L168

Savin, D. W. 1999, ApJ, 523, 855

Savin, D. W. 2000, ApJ, 533, 106

Savin, D. W., et al. 1997, ApJ, 489, L115

Savin, D. W., et al. 1999, ApJS, 123, 687

Savin, D. W., et al. 2002a, ApJS, 138, 337

Savin, D. W., et al. 2002b, ApJ, 576, 1098

Savin, D. W., et al. 2003, ApJS, 147, 421

Savin, D. W., et al. 2006, ApJ, 642, 1275

Schippers, S., Bartsch, T., Brandau, C., Gwinner, G., Linkemann, J., Müller, A., Saghiri, A. A., & Wolf, A. 1998, J. Phys. B, 31, 4873

Schippers, S., et al. 2000, Phys. Rev. A, 62, 022708

Schippers, S., Müller, A., Gwinner, G., Linkemann, J., Saghiri, A. A., & Wolf, A. 2001, ApJ, 555, 1027

Schippers, S., et al. 2002, Phys. Rev. A, 65, 042723

Schippers, S., Schnell, M., Brandau, C., Kieslich, S., Müller, A., & Wolf, A. 2004, A&A, 421, 1185

Schippers, S., et al. 2007, Phys. Rev. Lett., 98, 033001

Schmidt, E. W., et al. 2006, ApJ, 641, L157

Schnell, M., et al. 2003, Phys. Rev. Lett. 91, 043001

Schnell M., et al. 2003, Nucl. Instrum. Methods Phys. Res. B, 205, 367

Seaton, M. J., & Storey, P. J. 1976, in Atomic Processes and Applications, ed. P. G. Burke & B. L. Moisewitch (North-Holland, Amsterdam), 133

Sprenger, F., Lestinsky, M., Orlov, D. A., Schwalm, D., & Wolf, A. 2004, Nucl. Instrum. Methods Phys. Res. A, 532, 298

Steenbrugge, K. C., Kaastra, J. S., de Vries, C. P., & Edelson, R. 2003 A&A, 402, 477

Table 1. Energy levels for the $n = 3$ shell of Fe XV relative to the ground state.

Level	Energy (eV)[a]
$3s3p(^3P^o_0)$	28.9927
$3s3p(^3P^o_1)$	29.7141
$3s3p(^3P^o_2)$	31.4697
$3s3p(^1P^o_1)$	43.6314
$3p^2(^3P_0)$	68.7522
$3p^2(^1D_2)$	69.3816
$3p^2(^3P_1)$	70.0017
$3p^2(^3P_2)$	72.1344
$3p^2(^1S_0)$	81.7833
$3s3d(^3D_1)$	84.1570
$3s3d(^3D_2)$	84.2826
$3s3d(^3D_3)$	84.4848
$3s3d(^1D_2)$	94.4875
$3p3d(^3F^o_2)$	115.087
$3p3d(^3F^o_3)$	116.313
$3p3d(^3F^o_4)$	117.743
$3p3d(^1D^o_2)$	117.601
$3p3d(^3D^o_1)$	121.860
$3p3d(^3D^o_3)$	123.346
$3p3d(^3D^o_2)$	123.565
$3p3d(^3P^o_2)$	121.940
$3p3d(^3P^o_0)$	123.474
$3p3d(^3P^o_1)$	123.518
$3p3d(^1F^o_3)$	131.7351
$3p3d(^1P^o_1)$	133.2690
$3d^2(^3F_2)$	169.8994
$3d^2(^3F_3)$	170.1106
$3d^2(^3F_4)$	170.3612
$3d^2(^1D_2)$	173.8992
$3d^2(^1G_4)$	174.4529
$3d^2(^3P_0)$	174.2613[b]

Table 1—Continued

Level	Energy (eV)[a]
$3d^2(^3P_1)$	174.3433[b]
$3d^2(^3P_2)$	174.5416
$3d^2(^1S_0)$	184.3712

[a]Ralchenko et al. (2006) unless otherwise noted.

[b]Churilov et al. (1989)

Table 2. Measured resonance energies E_i and strengths S_i for Fe XV forming Fe XIV via $N = 3 \rightarrow N' = 3$ DR for $E_{\rm cm} \leq 0.95$. Fitting errors are presented at a 90% confidence level.

Peak Number	E_i (eV)	S_i (10^{-21} cm^2 eV)
1	(6.74 ± 0.05)E-3	189430.0 ± 20635.3
2	0.0098 ± 0.0008	10078.0 ± 483.1
3	0.0196 ± 0.0008	613.1 ± 56.8
4	0.0254 ± 0.0003	743.9 ± 51.8
5	0.0444 ± 0.0002	686.3 ± 37.9
6	0.0610 ± 0.0002	2949.3 ± 39.0
7	0.1098 ± 0.0002	805.5 ± 699.5
8	0.1674 ± 0.0014	2424.3 ± 954.1
9	0.1943 ± 0.0018	4408.5 ± 1213.1
10	0.2143 ± 0.0022	4735.5 ± 750.9
11	0.2436 ± 0.0003	4257.6 ± 132.6
12	0.2660 ± 0.0006	4169.1 ± 339.0
13	0.2895 ± 0.0122	213.9 ± 218.4
14	0.3102 ± 0.0074	292.5 ± 188.6
15	0.3346 ± 0.0008	1158.1 ± 118.6
16	0.3596 ± 0.0010	943.5 ± 100.3
17	0.4154 ± 0.0149	193.3 ± 230.2
18	0.4536 ± 0.0005	8013.6 ± 328.0
19	0.4781 ± 0.0072	706.9 ± 310.2
20	0.4988 ± 0.0072	781.3 ± 303.5
21	0.5199 ± 0.0266	216.7 ± 285.6
22	0.5433 ± 0.0290	121.8 ± 270.4
23	0.6164 ± 0.0078	136.2 ± 106.9
24	0.6599 ± 0.0006	1269.1 ± 97.8
25	0.6992 ± 0.0010	3090.3 ± 99.5
26	0.7385 ± 0.0010	2068.5 ± 113.4
27	0.7943 ± 0.0006	1594.4 ± 83.7
28	0.8406 ± 0.0006	1740.6 ± 83.6
29	0.8830 ± 0.0006	2164.2 ± 89.9
30	0.9232 ± 0.0013	1420.7 ± 86.9

Table 3. Fit parameters for the total experimentally-derived DR rate coefficient for Fe XV forming Fe XIV via $N = 3 \rightarrow N' = 3$ core excitation channels and including the theoretical estimate for capture into $n > 80$ ($n_{\max} = 1000$). See § 4 for an explanation of the columns labeled "Experiment (I)" and "Experiment (II)". Also given are the fit parameters for our calculated MCBP results ($n_{\max} = 1000$). The units below are cm^3 s^{-1} K$^{1.5}$ for c_i and eV for E_i.

Parameter	Experiment (I)	Experiment (II)	MCBP
c_1	1.07E-4	1.07E-4	7.07E-4
c_2	8.26E-6	8.26E-6	7.18E-3
c_3	1.00E-6	1.00E-6	2.67E-2
c_4	1.46E-6	1.46E-5	3.15E-2
c_5	2.77E-6	2.77E-6	1.62E-1
c_6	1.51E-5	1.51E-6	5.37E-4
c_7	2.90E-6	3.29E-6	-
c_8	2.66E-5	1.63E-4	-
c_9	5.62E-5	4.14E-4	-
c_{10}	6.66E-5	2.17E-3	-
c_{11}	6.81E-5	6.40E-3	-
c_{12}	7.28E-5	4.93E-2	-
c_{13}	4.07E-6	1.51E-1	-
c_{14}	5.96E-6	-	-
c_{15}	2.54E-5	-	-
c_{16}	2.23E-5	-	-
c_{17}	5.27E-6	-	-
c_{18}	2.40E-4	-	-
c_{19}	2.22E-5	-	-
c_{20}	2.56E-5	-	-
c_{21}	7.40E-6	-	-
c_{23}	4.35E-6	-	-
c_{23}	5.51E-6	-	-
c_{24}	5.50E-5	-	-
c_{25}	1.42E-4	-	-
c_{26}	1.00E-4	-	-
c_{27}	8.32E-5	-	-
c_{28}	9.61E-5	-	-
c_{29}	1.25E-4	-	-
c_{30}	8.61E-5	-	-
c_{31}	1.02E-4	-	-

Table 3—Continued

Parameter	Experiment (I)	Experiment (II)	MCBP
c_{32}	5.46E-1	-	-
c_{33}	2.91E-3	-	-
c_{34}	4.83E-3	-	-
c_{35}	4.86E-2	-	-
c_{36}	1.51E-1	-	-
E_1	6.74E-3	6.74E-3	4.12E-1
E_2	9.80E-3	9.80E-3	2.06E+0
E_3	1.97E-2	1.97E-2	1.03E+1
E_4	2.54E-2	2.54E-2	2.20E+1
E_5	4.45E-2	4.45E-2	4.22E+1
E_6	6.10E-2	6.10E-2	3.41E+3
E_7	1.10E-1	1.10E-1	-
E_8	1.67E-1	1.91E-1	-
E_9	1.94E-1	3.33E-1	-
E_{10}	2.14E-1	9.63E-1	-
E_{11}	2.44E-1	2.47E+0	-
E_{12}	2.66E-1	1.08E+1	-
E_{13}	2.90E-1	3.83E+1	-
E_{14}	3.10E-1	-	-
E_{15}	3.35E-1	-	-
E_{16}	3.60E-1	-	-
E_{17}	4.15E-1	-	-
E_{18}	4.54E-1	-	-
E_{19}	4.78E-1	-	-
E_{20}	4.99E-1	-	-
E_{21}	5.20E-1	-	-
E_{22}	5.43E-1	-	-
E_{23}	6.16E-1	-	-
E_{24}	6.60E-1	-	-
E_{25}	6.99E-1	-	-

Table 3—Continued

Parameter	Experiment (I)	Experiment (II)	MCBP
E_{26}	7.39E-1	-	-
E_{27}	7.94E-1	-	-
E_{28}	8.41E-1	-	-
E_{29}	8.83E-1	-	-
E_{30}	9.23E-1	-	-
E_{31}	1.00E+0	-	-
E_{32}	1.16E+0	-	-
E_{33}	1.62E+0	-	-
E_{34}	3.14E+0	-	-
E_{35}	1.08E+1	-	-
E_{36}	3.82E+1	-	-

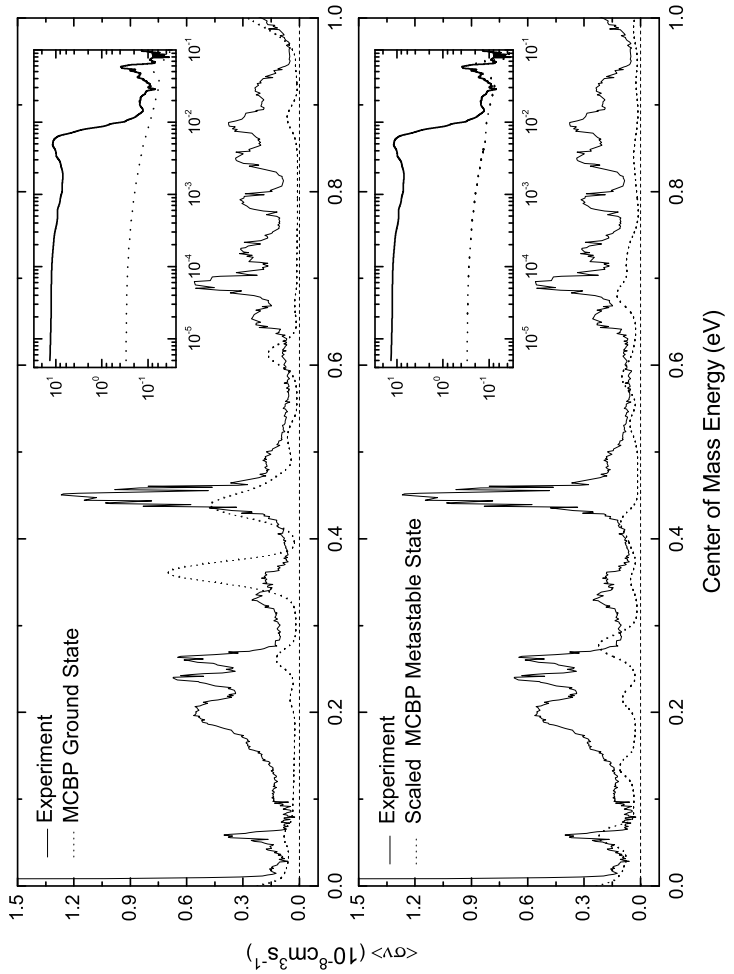

Fig. 1.— Fe XV to Fe XIV 3 → 3 DR resonance structure versus center-of-mass energy $E_{\rm cm}$ from 0 to 1 eV. The *solid curve* represents the measured rate coefficient $\langle \sigma v \rangle$ which is the summed DR plus radiative recombination (RR) cross sections times the relative velocity convolved with the experimental energy spread, i.e., a merged beam recombination rate coefficient (MBRRC). The *dotted curve* shows our calculated multiconfiguration Breit-Pauli (MCBP) results ($n_{\rm max} = 80$) for ground state Fe XV (top plot) and $^3P_0$ metastable state Fe XV multiplied by a factor of 0.06 to account for the estimated 6% population in our ion beam (bottom plot). To these results we have added the convolved, non-resonant RR contribution obtained from semi-classical calculations (Schippers et al. 2001). The inset shows our results for $E_{\rm cm}$ from 5×10^{-6} to 1×10^{-1} eV.

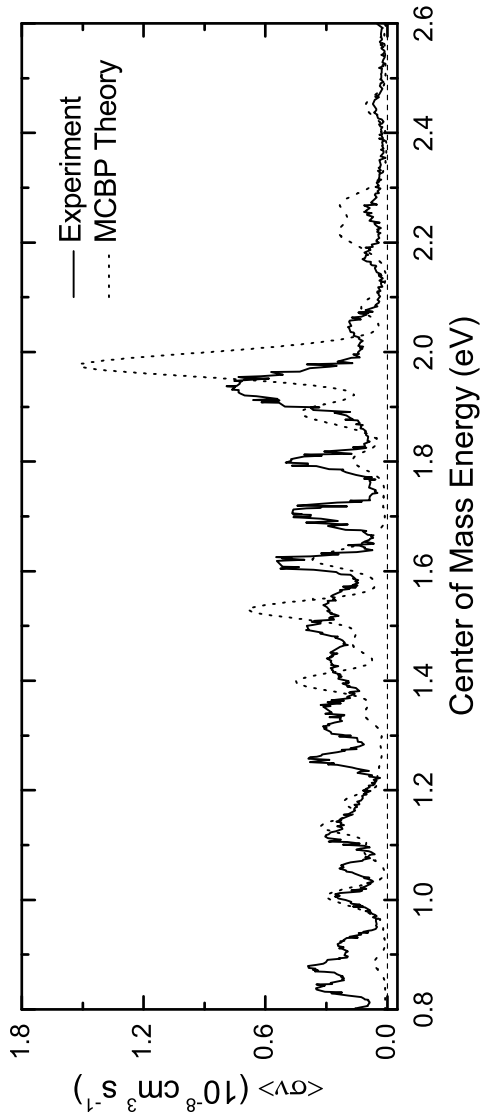

Fig. 2.— Same as Fig. 1 but only for ground state Fe XV from 0.8 to 2.6 eV.

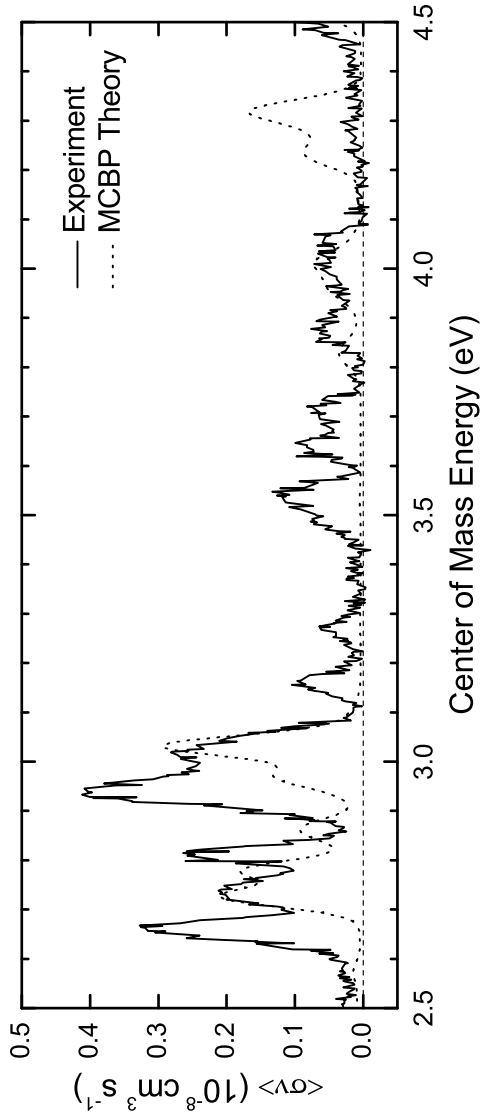

Fig. 3.— Same as Fig. 2 but for $E_{\rm cm}$ from 2.5 to 4.5 eV.

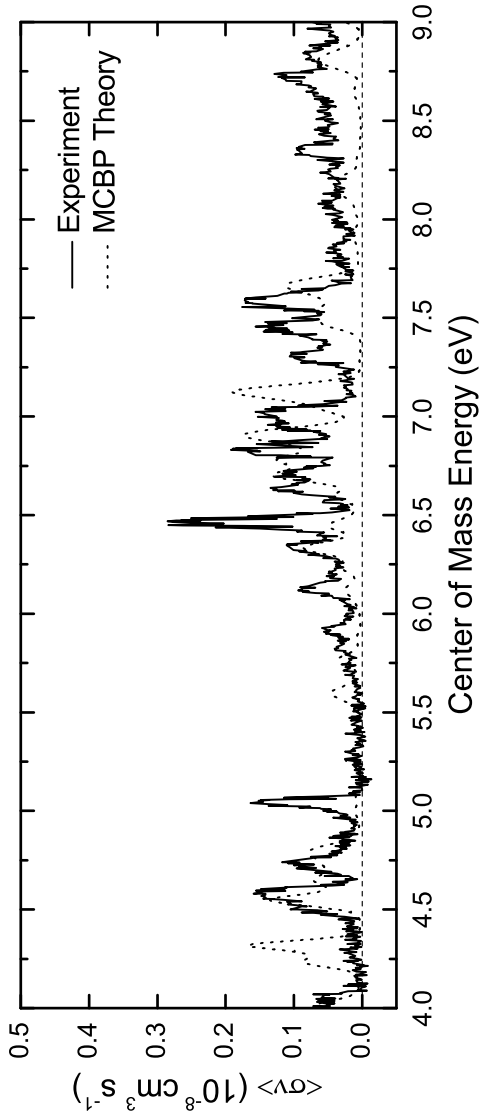

Fig. 4.— Same as Fig. 2 but for $E_{\rm cm}$ from 4 to 9 eV.

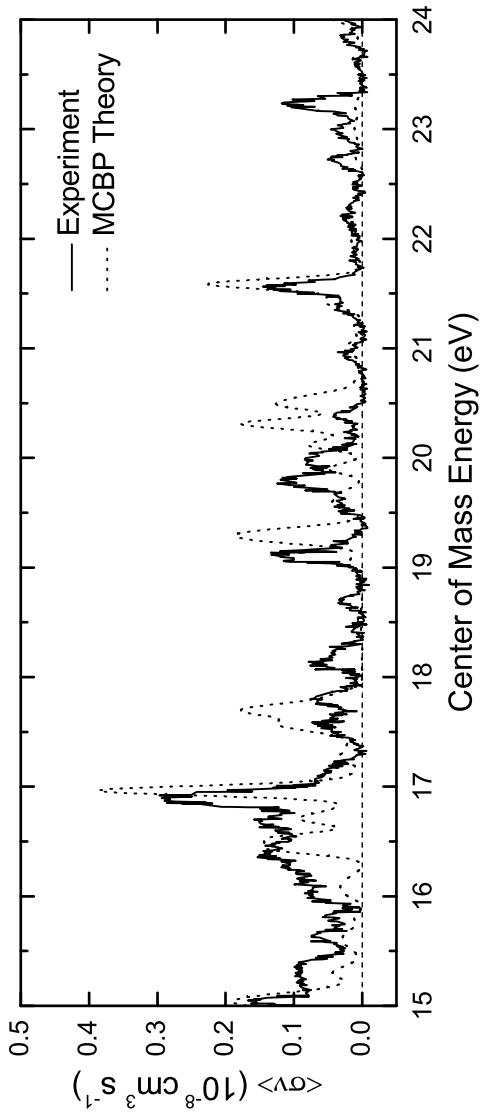

Fig. 5.— Same as Fig. 2 but for $E_{\rm cm}$ from 8 to 16 eV.

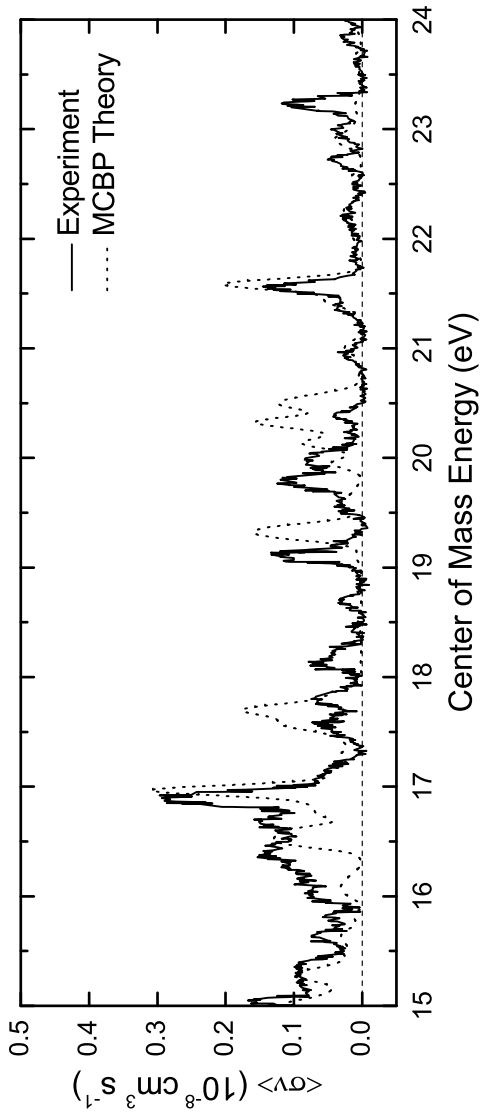

Fig. 6.— Same as Fig. 2 but for $E_{\rm cm}$ from 15 to 24 eV.

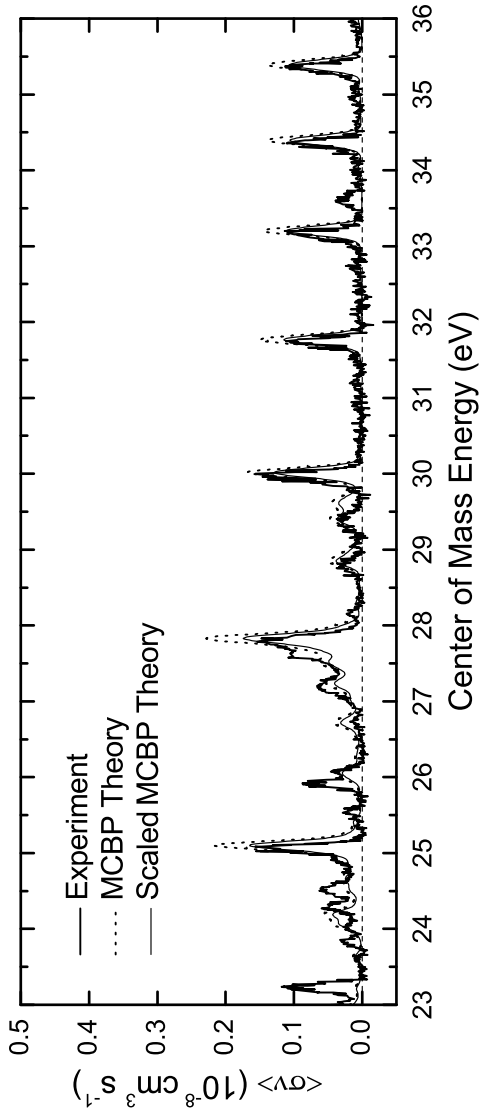

Fig. 7.— Same as Fig. 2 but for $E_{\rm cm}$ from 23 to 36 eV. The *dotted curve* shows our calculated MCBP results and the *thin solid curve* shows our calculated MCBP results reduced by a factor of 1.31.

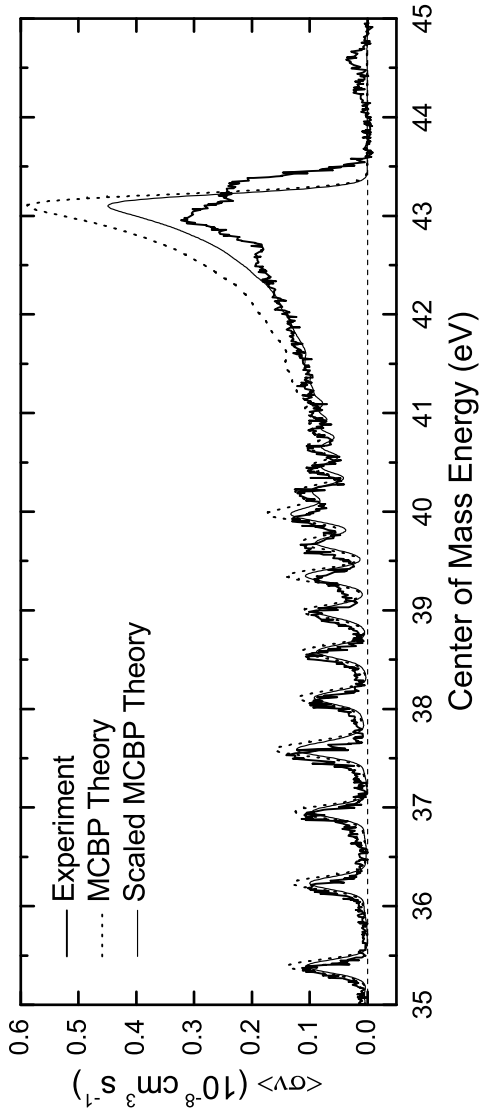

Fig. 8.— Same as Fig. 7 but for $E_{\rm cm}$ from 35 to 45 eV. The weak resonances above 44 eV are attributed to ΔN=1 DR. These are not included in either our experimentally-derived or theoretical Maxwellian rate coefficients.

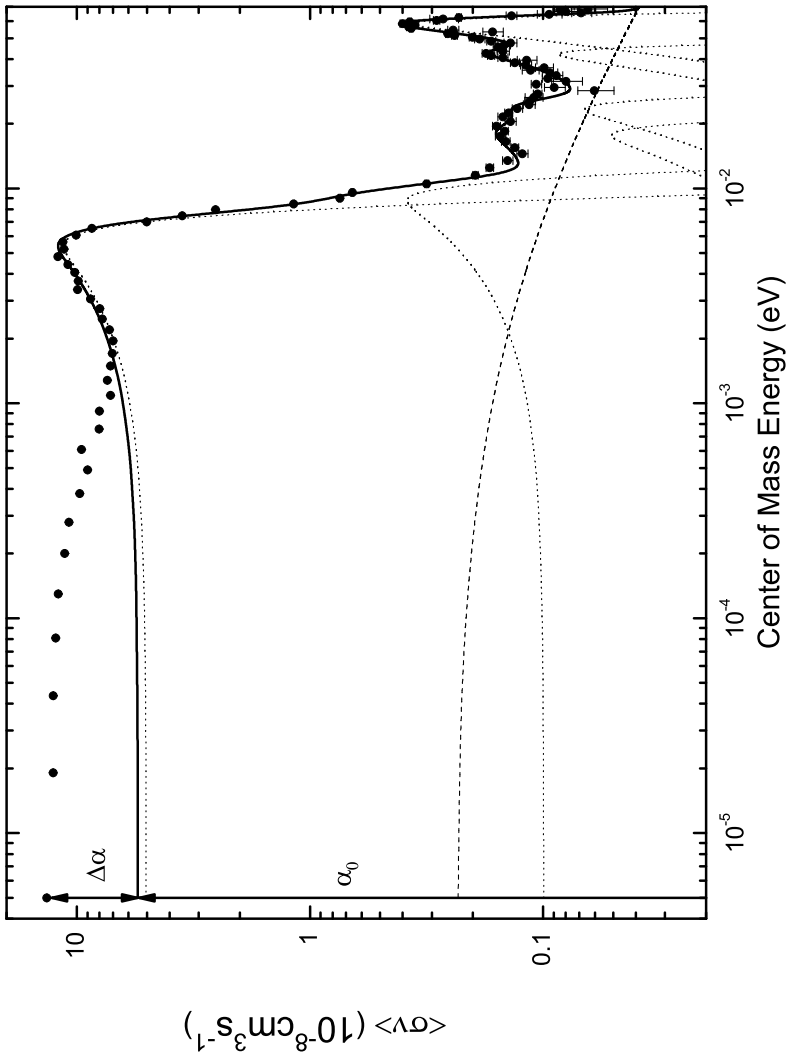

Fig. 9.— Measured and fitted Fe XV to Fe XIV $3 \rightarrow 3$ resonance structure below 0.07 eV. The experimental MBRRC results are shown by the *filled circles*. The vertical error bars show the statistical uncertainty of the data points. The *solid curve* is the fit to the data using our calculated RR rate coefficient (*dashed curve*) and taking into account all resolved DR resonances. The *dotted curves* show the fitted DR resonances. At $E_{\rm cm} = 0.005$ meV the difference between the model spectrum α_0 and the data is $1 + (\Delta\alpha/\alpha_0) = 2.5$.

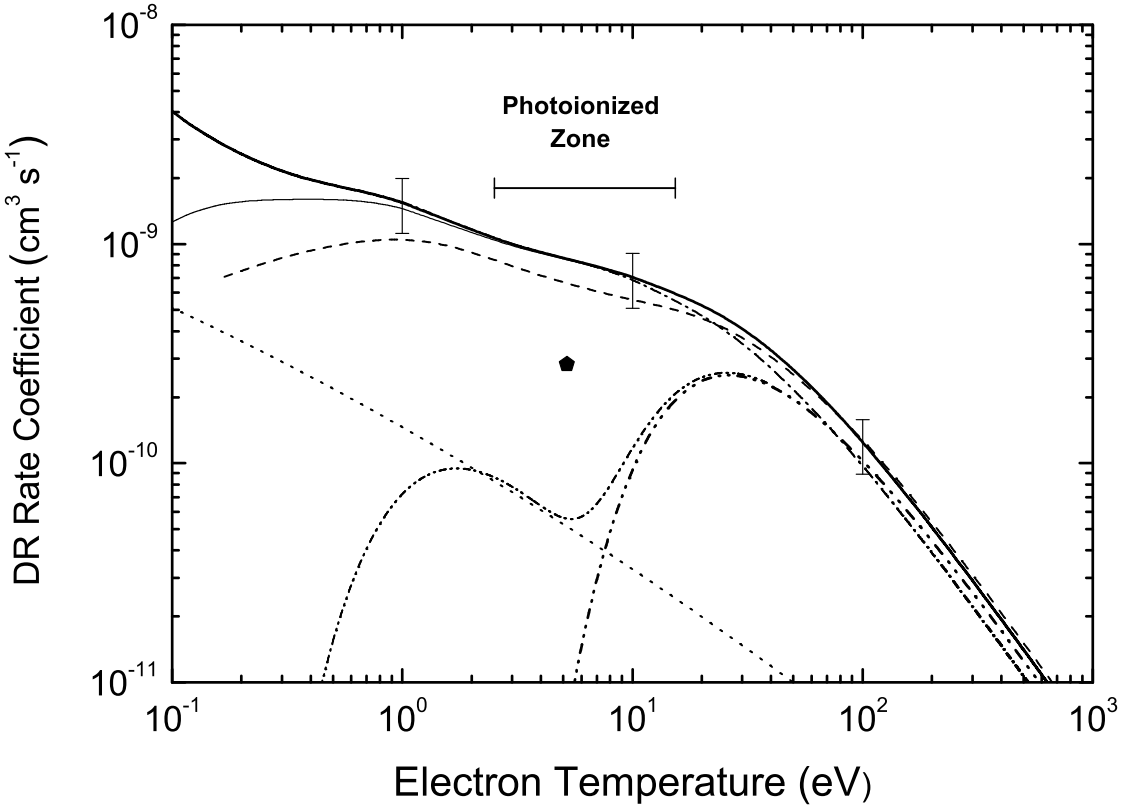

Fig. 10.— Maxwellian-averaged $3 \rightarrow 3$ DR rate coefficients for Fe XV forming Fe XIV. The *solid curve* represent our experimentally-derived rate coefficient plus the theoretical estimate for unmeasured contributions due to capture into states with $n > 80$. The error bars show our estimated total experimental uncertainty of ±29% (at a 90% confidence level). No error bars are shown below 1 eV for reasons discussed in § 4. The *thin solid curve* represents our experimentally-derived rate coefficient without the two lowest energy resonances included. The *dash-dotted curve* represents our experimentally-derived rate coefficient alone ($n_{\rm max} = 80$). Also shown is the recommended DR rate coefficient of Arnaud & Raymond (1992; *thick dash-dot-dotted curve*) and its modification by Netzer (2004; *thin dash-dot-dotted curve*). The *filled pentagon* at 5.2 eV represents the estimated rate coefficient from Kraemer et al. (2004). The *dashed curve* shows our MCBP calculations for $n_{\rm max} = 1000$. As a reference we show the recommended RR rate coefficient of Arnaud & Raymond (1992; *dotted curve*). Neither the experimental nor theoretical DR rate coefficients include RR. The horizontal line shows the temperature range over which Fe XV is predicted to form in photoionized gas (Kallman & Bautista 2001).